# Density-dependent electronic structure of zinc-blende-type MnAs dots on GaAs(001) studied by *in situ* photoemission spectroscopy

J. Okabayashi,[1,*] M. Mizuguchi,[2] K. Ono,[3] M. Oshima,[1] A. Fujimori,[4] H. Kuramochi,[2] and H. Akinaga[2]
[1]*Department of Applied Chemistry, The University of Tokyo, Bunkyou-ku 113-8656, Japan*
[2]*National Institute of Advanced Industrial Science and Technology (SYNAF-AIST), Tsukuba, Ibaraki 305-8562, Japan*
[3]*Institute of Materials Structure Science, KEK, Tsukuba, Ibaraki 305-0801, Japan*
[4]*Department of Complexity Science and Engineering, The University of Tokyo, Kashiwa 277-8561, Japan*
(Received 9 September 2004; published 9 December 2004)

We report on the density dependence of the morphology and electronic structure of zinc-blende-type MnAs dots using *in situ* photoemission spectroscopy combined with molecular-beam epitaxy. Transmission electron microscopy images showed the zinc-blende-type crystalline structure of 10-nm diameter for each dot on sulfur-passivated GaAs(001) surface. The valence-band photoemission spectra of the MnAs dots were similar to those of the diluted magnetic semiconductor $Ga_{1-x}Mn_xAs$. With increasing dot density, the characteristic spectra of the zinc-blende-type MnAs persist but a weak Fermi edge appears, suggesting a metallic behavior as a result of percolation between the dots or the appearance of hexagonal MnAs as a minority phase.

DOI: 10.1103/PhysRevB.70.233305 PACS number(s): 73.22.−f, 75.50.Pp, 79.60.Jv

The successful synthesis of the diluted magnetic semiconductor (DMS) $Ga_{1-x}Mn_xAs$ epitaxially grown on GaAs substrates using molecular-beam epitaxy (MBE) has opened up the semiconductor spin-electronics research field, because it has a large number of functionalities that can be utilized as nonvolatile memories, spin injection, and optical control of ferromagnetism in semiconductor devices.[1] However, the Curie temperature ($T_C$) has been mostly limited to ~110 K, because of the solubility limit of Mn atoms and the selfcompensation of doped carriers.[2] Recently, considerable effort has been devoted to raise the $T_C$ of $Ga_{1-x}Mn_xAs$ as in Mn $\delta$ doping in GaAs and MnAs/GaAs multilayers.[3–5] To this end, there is a strong demand for the fabrication of the high-Mn-concentration limit of $Ga_{1-x}Mn_xAs$, namely, MnAs with the zinc-blende-type structure, which has a high potential for a breakthrough toward GaAs-compatible materials with a higher $T_C$.[6] However, it is well known that MnAs grows epitaxially onto GaAs in the hexagonal NiAs-type structure.[7] This is because the MnAs/GaAs interfaces are thermodynamically stable as both materials share As atoms at the interface and the growth process is completely compatible with the existing III-V MBE technology.

In the previous work, we have reported a fabrication of the zinc-blende-type MnAs nanoscale dots on sulfur-passivated GaAs(001).[8] Fabrication of thicker films of the zinc-blende-type MnAs is strongly anticipated because of its half-metallic behavior as suggested by hypothetical band-structure calculations.[9–13] However, it has been suspected that thick films may have the crystalline structure of the thermodynamically stable NiAs-type bulk MnAs because of lattice relaxation.[7] The precise information on the density dependence of the structural and electronic properties of the MnAs dots on GaAs is therefore strongly required for the fabrication of thicker zinc-blende-type MnAs films. It was proposed that MnSb dots on sulfur-passivated GaAs surface maintain the NiAs-type structure because of the lattice mismatch between the zinc-blende-type MnSb and GaAs substrates.[14] On the other hand, zinc-blende-type CrAs can be grown on GaAs below a critical thickness of 3 nm because of the small lattice mismatch.[15] As the lattice mismatch between MnAs and GaAs is intermediate between the above two systems, a detailed investigation is needed to see how MnAs dots are grown on GaAs surface. In this paper, we report on the morphology-dependent, especially dot-density dependent, photoemission spectroscopy of the zinc-blende-type MnAs dots on GaAs(001) using an *in situ* photoemission spectroscopy system combined with a MBE system.

The nanoscale MnAs dots were fabricated on sulfur-passivated $n^+$-GaAs(001) substrates by a conventional solid-source MBE. It is well known that the GaAs substrates terminated by group VI-element atoms, such as sulfur and selenium, have a low surface energy, and thus enable a self-assembled growth of metallic clusters on the semiconductor.[16] To terminate the surface of GaAs substrates by sulfur, the substrate was first dipped into an $(NH_4)_2S_x$ solution for 1 h, then rinsed in pure water. By heating the substrates up to 400 °C, the reflection high-energy electron diffraction (RHEED) pattern changed from a halo to a streaky $1\times1$ pattern, indicating the formation of flat surfaces. The growth of MnAs dots changed the streaky $1\times1$ RHEED pattern to a spotty pattern, indicating the dot formation. The growth temperature of the MnAs dots on the substrate was set at 200 °C. As references, we have grown $Ga_{1-x}Mn_xAs$ and NiAs-type MnAs film on GaAs(001) by the same recipes as reported in Refs. 1 and 7.

For the investigations of the density dependence of the MnAs dots, we prepared three samples with different dot densities of 3.5, 2.0, and $1.5\times10^{12}$ $cm^{-2}$ deduced from the analysis of the atomic force microscopy (AFM) images as shown in Fig. 1(a). Hereafter we refer to the three samples as high-, medium-, and low-density samples. For all the samples, the maximum diameter and the maximum height of each dot were estimated to be about 10 and 5 nm, respectively. For sizes larger than 10 nm in diameter, new dots were formed in other areas of the sulfur-terminated GaAs substrate. In the case of the high-density sample, AFM im-

 

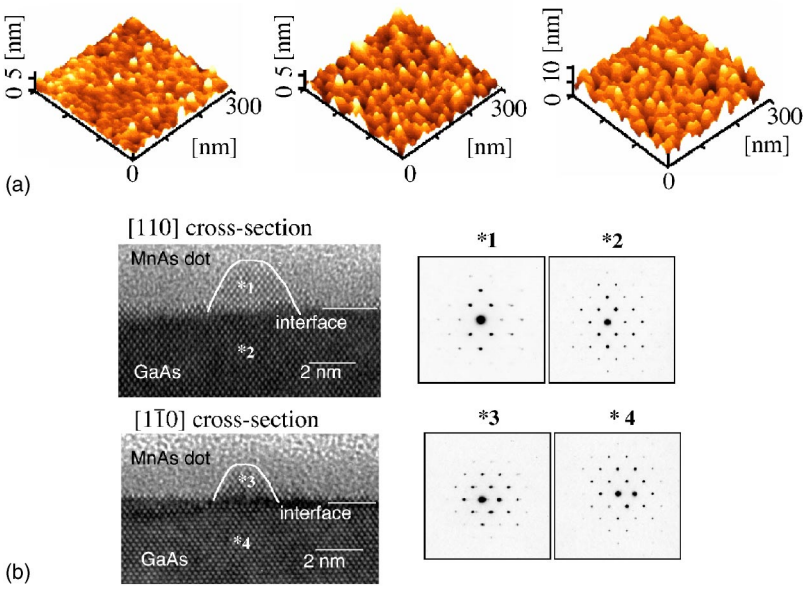


FIG. 1. (Color online) Density-dependent surface morphology of the nanoscale MnAs dots. (a) Atomic force microscopy images for different dot densities in $300\times300$ nm$^2$; low density (left), medium density (middle), and high density (right). (b) Cross-sectional transmission electron microscopy (TEM) images of the zinc-blende-type MnAs dots in medium density along the [110] and [1$\bar{1}$0] directions. Selected area electron diffraction patterns for each place are also shown in the right panel.

ages reveal that the MnAs dots are connected with each other. In fact, the root-mean-square value in the high-density sample was larger than those of medium- and low-density samples. Therefore, with increasing deposition time, the size of the dots remained almost constant ~10 nm and the dot densities increased because of the low surface energy of the sulfur-passivated surface.[16]

In the transmission electron microscopy (TEM) images shown in Fig. 1(b), clear lattice fringes of the nanoscale MnAs dots as well as the GaAs substrate are observed for both the [110] and [1$\bar{1}$0] cross sections. The dark contrast in the interface region is due to the sulfur layer at the interface. The lattice images and selected area electron diffraction patterns of the nanoscale MnAs dots also shown in Fig. 1(b) are almost the same as those of the GaAs substrate, indicating the formation of the zinc-blende crystalline structure in the nanoscale MnAs dots. The lattice constant of the zinc-blende-type MnAs dots was larger by 0.7% than the lattice constant 5.65 Å of the GaAs substrate. Without the sulfur passivation, the crystalline structure, observed by the high-resolution TEM, of the MnAs film on GaAs(001) was different from that of the GaAs substrate, indicating that the MnAs film was grown in the hexagonal NiAs-type crystalline structure.[18] The zinc-blende-type MnAs dots observed here are not the same as the high Mn concentration limit of $Ga_{1-x}Mn_xAs$ in the sense that the linear extrapolation to $x\rightarrow1$ would yield $a=5.75$ Å and a considerably large lattice mismatch of 5.8% with the GaAs substrate would be expected. It is considered that the formation of the zinc-blende-type structure and the small lattice mismatch in the nanoscale MnAs dots result from the strong Mn-S bond compared to the Mn-As bond inferred from the heats of formation of MnS and MnAs. Therefore, the nanoscale MnAs dots maintain the zinc-blende-type structure through the interaction with the sulfur-terminated layer. It is also noted that in the case of the nanoscale MnSb dots on sulfur-passivated GaAs surface, they form in the hexagonal crystalline structure, which has been attributed to the large lattice mismatch with the GaAs substrate.[14]

The MBE system used in this study was connected to the synchrotron radiation photoemission system at BL-1C (Ref. 17) of the Photon Factory, High-Energy Accelerator Research Organization (KEK) in Japan. *In situ* photoemission spectroscopy measurements were performed for the MBE-grown MnAs dots. The samples grown by MBE were transferred into the photoemission chamber without breaking the ultrahigh vacuum. The emission angle of photoelectrons was set normal to the surface. Photoemission measurements were done at room temperature and the total-energy resolution was set at about 100 meV using a Gammadata-Scienta SES-100 hemispherical analyzer. The AFM and TEM measurements were made after the photoemission measurement.

The Mn 3*d* partial density of states (PDOS) of the nanoscale MnAs dots has been obtained using the $3p-3d$ resonant photoemission spectroscopy and is compared with those of $Ga_{1-x}Mn_xAs$ and NiAs-type MnAs film in Fig. 2. The Mn 3*d* PDOS has been deduced by the subtraction of the photoemission spectrum taken at 48 eV from that taken at 50 eV. Figure 2(a) shows the valence-band photoemission spectra of the *in situ* prepared $Ga_{1-x}Mn_xAs$. The Mn 3*d* PDOS of $Ga_{1-x}Mn_xAs$ is similar to that reported previously.[19] Resonant enhancement was observed in the photoemission spectra taken at 50 eV from $E_F$ to ~−10 eV with a prominent peak at ~−4 eV. $Ga_{1-x}Mn_xAs$ has the zinc-blende-type crystalline structure with the Mn atom tetrahedrally coordinated by As atoms. All the tetrahedrally bonded Mn-based DMS including II-VI compounds reported so far show almost the same Mn 3*d* PDOS, that is, the main peak located around −4 eV, a strong satellite structure at deep energies around −7~−9 eV, and a relatively small spectral weight within −2 eV from $E_F$.[20] Such an electronic structure has been well understood using the configuration-interaction cluster model and cannot be reproduced within the framework of band-structure calculations, indicating the importance of the Coulomb interaction between the Mn 3*d* electrons.[20] On the other hand, the photoemission spectra of the MnAs film in Fig. 2(d) do not show the pronounced −4 eV peak or the satellite structure in the on resonance ($h\nu\sim50$ eV) but show

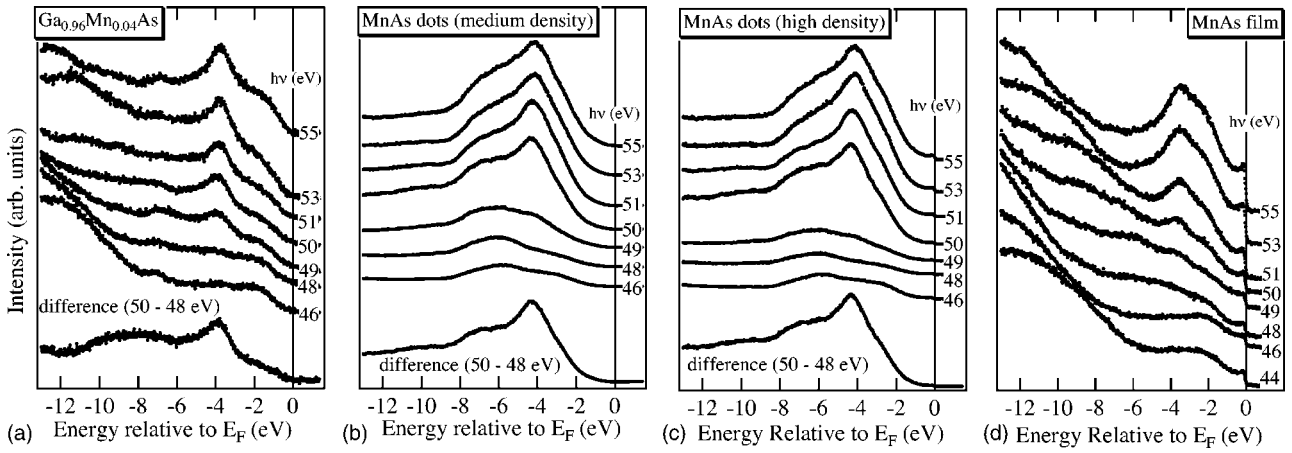


FIG. 2. A series of valence-band photoemission spectra, in the Mn $3p-3d$ core excitation threshold, of *in situ* prepared $Ga_{1-x}Mn_xAs$ (a), the zinc-blende-type MnAs dots in the middle density (b), the zinc-blende-type MnAs dots in the high density (c), and NiAs-type MnAs film (d). The difference spectra between the on-resonance ($h\nu$=50 eV) and off-resonance (48 eV) spectra are also shown at the bottom of each panel as a measure of the Mn 3*d* partial density of states.

a clear Fermi edge characteristic of a metallic material. A strong Auger structure from the As 3*d* core level as well as Mn $3p-3d-3d$ also overlap the valence-band spectra, which suggests the itinerant character of the valence electrons.

Resonant photoemission spectra of the nanoscale MnAs dots are shown in Figs. 2(b) and 2(c) for the medium- and high-density dots, respectively. The spectra of the low-density MnAs dots (not shown) show almost the same feature as those of the medium-density MnAs dots. Spectral line shapes in the entire valence-band region are similar to those of $Ga_{1-x}Mn_xAs$, but are quite different from the photoemission spectra of the NiAs-type MnAs films, even in the high-density MnAs dots. The distance between Mn atoms in the zinc-blende-type MnAs is much larger than that in the NiAs-type MnAs, and therefore the Mn 3*d* electrons have tendency to be strongly correlated. This is indicated by the strong satellite structure in the valence band and the similar photoemission spectra of $Ga_{1-x}Mn_xAs$ in which doped Mn atoms behave as impurities. Therefore, the similarity in the line shapes between the MnAs dots and $Ga_{1-x}Mn_xAs$ is considered to be derived from the zinc-blende-type structure and the strong correlation among the Mn 3*d* electrons. The absence of the As-derived and Mn-derived Auger emission in the spectra of the MnAs dots would be explained by the strong tendency toward the localization of the hybridized Mn 3*d*-As 4*p* states.

Although one may suspect the MnS formation between the substrate and the dots, or on the surface of the dots, we have confirmed the diminishing intensity of the S 2*p* core-level peak with increasing the MnAs dot densities as shown in Fig. 3, where the spectra have been normalized to the As 3*d* peak height. Since the photoionization cross sections of the As 3*d* and S 2*p* orbitals are comparable, only a small amount of Mn-S bonds can exist in the interface region.

To see this more clearly, in Fig. 3, we show five spectra of the zinc-blende-type MnAs dots with different dot densities taken at 80-eV photon energy, where the relative photoionization cross sections of Mn 3*d* to As 4*p* increase. The spectra have been normalized to the As 3*d* core-level height. With increasing dot density, the Fermi edge appears at the density of $3\times10^{12}$ cm$^{-2}$ and grows gradually. Except for the evolution of the Fermi edge, the entire valence band shows almost the same spectral line shapes, which indicates that the formation of the zinc-blende-type MnAs dominates up to the high-density region. The main peak positions at around $-4.5$ eV are consistent with the previous studies of ultrathin Mn layers on GaAs(001) substrates forming the fcc structure since the $\alpha$-phase Mn layer showed the main peak position at $-3$ eV below $E_F$.[21] Spectra of the high-density MnAs dots show a clear Fermi edge. The appearence of the Fermi edge for the high-density dots suggests that a small amount of NiAs-type MnAs starts to form at this dot density or that the dots are contacted by each other and a conductive pass appears by percolation between dots, resulting in the occurrence of an insulator-to-metal transition. The latter scenario is consistent with the AFM observation shown in Fig. 1(a).

The insulator-to-metal transition is also expected to influence the magnetic properties. Since the samples are thin

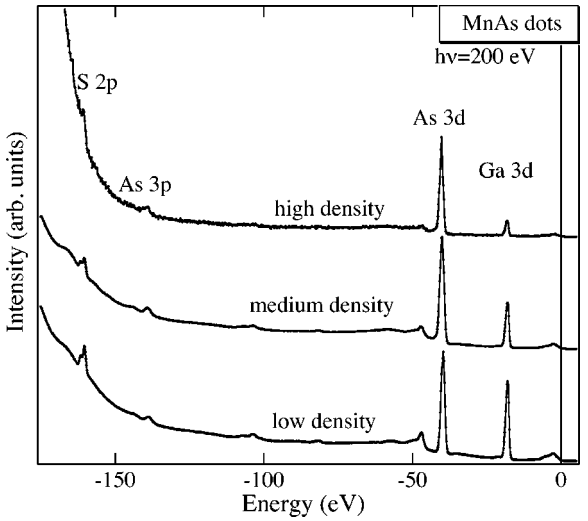


FIG. 3. Wide-range photoemission spectra of the nanoscale MnAs dots for different dot densities.

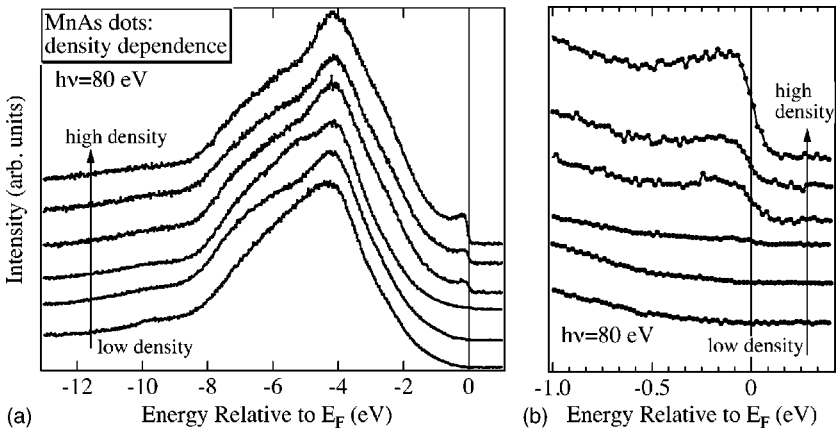


FIG. 4. Dot-density-dependent photoemission spectra of the zinc-blende-type MnAs dots taken at 80-eV photon energy. (a) Entire valence-band spectra and (b) narrow range spectra near the Fermi level.

films and the magnetic atoms are dilute, it is difficult to characterize the magnetic properties using conventional magnetic measurements. In the magnetic circular dichroism study in the Mn 2*p* core-level absorption,[22] it was revealed that the high-density samples behave ferromagnetically, although the samples with dot density less than the percolation density ($3\times10^{12}$ cm$^{-2}$) show nonferromagnetic (superparamagnetic) behavior. According to the band-structure calculation, the zinc-blende-type MnAs is predicted to be a half-metallic ferromagnet.[9–13] If the metallic and ferromagnetic high-density MnAs dots behave as a half metal, they will become a useful material for spintronic device application in future.

In conclusion, we have investigated the electronic structure of the zinc-blende-type MnAs dots using the *in situ* photoemission system combined with MBE focusing on its dot-density dependence. The valence-band photoemission spectra of the MnAs dots were similar to those of $Ga_{1-x}Mn_xAs$. An insulator-to-metal transition was observed, which we attribute to a percolation between the dots or the NiAs-type MnAs formation as a minority phase.

This work was done under the project 02S2-002 at the Institute of Materials Structure Science in KEK, and partially supported by the New Energy and Industrial Technology Development (NEDO) and a Grant-in-Aid for Scientific Research in Priority Area Semiconductor Nano-spintronics from the Ministry of Education, Culture, Sports, Science and Technology.

*Author to whom correspondence should be addressed. Email address: jun@sr.t.u-tokyo.ac.jp

[1] H. Ohno, A. Shen, F. Matsukura, A. Oiwa, A. Endo, S. Katsumoto, and Y. Iye, Appl. Phys. Lett. **69**, 363 (1996);
[2] T. Dietl, H. Ohno, and F. Matsukura, Phys. Rev. B **63**, 195205 (2001).
[3] Ahsan M. Nazmul, S. Sugawa, and M. Tanaka, Appl. Phys. Lett. **80**, 3120 (2002).
[4] R. K. Kawakami, E. J. Halperin, L. F. Chen, M. Hanson, N. Guebels, J. S. Speck, A. C. Gossard, and D. D. Awshalom, Appl. Phys. Lett. **77**, 2379 (2000).
[5] Y. L. Soo, G. Kioseoglou, S. Kim, X. Chen, H. Luo, Y. H. Kao, Y. Sasaki, X. Liu, and J. K. Furdyna, Appl. Phys. Lett. **80**, 2654 (2002).
[6] K. Sato and H. Katayama-Yoshida, Europhys. Lett. **61**, 403 (2003).
[7] M. Tanaka, J. P. Habrison, M. C. Park, Y. S. Park, T. Shin, and G. M. Rothberg, Appl. Phys. Lett. **65**, 1964 (1994); M. Tanaka, Semicond. Sci. Technol. **17**, 327 (2002).
[8] K. Ono, J. Okabayashi, M. Mizuguchi, M. Oshima, A. Fujimori, and H. Akinaga, J. Appl. Phys. **91**, 8088 (2002).
[9] M. Shirai, T. Ogawa, I. Kitagawa, and N. Suzuki, J. Magn. Magn. Mater. **177-181**, 1383 (1998).
[10] S. Sanvito and N. A. Hill, Phys. Rev. B **62**, 15 553 (2000).
[11] A. Continenza, S. Picozzi, W. T. Geng, and A. J. Freeman, Phys. Rev. B **64**, 085204 (2001).
[12] I. Galanakis and P. Mavropoulos, Phys. Rev. B **67**, 104417 (2003).
[13] A. Janotti, S.-H. Wei, and L. Bellaiche, Appl. Phys. Lett. **82**, 766 (2003).
[14] H. Akinaga, M. Mizuguchi, K. Ono, and M. Oshima, Appl. Phys. Lett. **76**, 357 (2000).
[15] H. Akinaga, T. Manago, and M. Shirai, Jpn. J. Appl. Phys., Part 1 **39**, 1118 (2000).
[16] M. Sugiyama, N. Yabumoto, S. Maeyama and M. Oshima, Jpn. J. Appl. Phys., Part 1 **34**, L1588 (1995); N. Koguchi and K. Ishige, *ibid.* **32**, 2052 (1993).
[17] K. Ono, J.-H. Oh, K. Horiba, M. Mizuguchi, M. Oshima, T. Kiyokura, F. Maeda, Y. Watanabe, A. Kakizaki, T. Kikuchi, A. Yagishita, and H. Kato, Nucl. Instrum. Methods Phys. Res. A **467-468**, 573 (2001).
[18] A. Trampert, F. Schippan, L. Daweritz, and K. H. Ploog, Appl. Phys. Lett. **78**, 2461 (2001).
[19] J. Okabayashi, A. Kimura, T. Mizokawa, A. Fujimori, T. Hayashi, and M. Tanaka, Phys. Rev. B **59**, R2486 (1999).
[20] T. Mizokawa and A. Fujimori, Phys. Rev. B **48**, 14 150 (1993).
[21] X. Jin, M. Zhang, G. S. Dong, Y. Chen, M. Xu, X. G. Zhu, X. Wang, E. D. Lu, H. B. Pan, P. S. Xu, X. Y. Zhang, and C. Y. Fan, Phys. Rev. B **50**, 9585 (1994).
[22] J. Okabayashi, M. Mizuguchi, K. Ono, M. Oshima, A. Fujimori, M. Yuri, C. T. Chen, and H. Akinaga, J. Magn. Magn. Mater. **272-276**, 1553 (2004).